NeuroImage **9,** 407–415 (1999)
Article ID nimg.1998.0424, available online at http://www.idealibrary.com on IDEAL®

Localization of Cardiac-Induced Signal Change in fMRI

Mandeep S. Dagli, John E. Ingeholm, and James V. Haxby

Laboratory of Brain and Cognition, NIMH, National Institutes of Health, Bethesda, Maryland 20892

Received May 19, 1998

Signal detection in the analysis of blood oxygen level-dependent (BOLD) functional magnetic resonance imaging (fMRI) may be greatly hindered by cardiac pulsatility artifacts. Vessel pulsation, cerebrospinal fluid movement, and tissue deformation are all associated with the cardiac cycle and all can produce fMRI signal variance. Most cognitive fMRI studies do not utilize a method of cardiac-related noise reduction, in part because of the lack of information on the regional significance and magnitude of cardiac-related signal variance in the brain. In this paper we present a topographical description of the regions showing significant contributions of cardiac-related signal variance. The results are highly consistent across subjects and suggest that reduced sensitivity due to cardiac-induced noise in the BOLD signal is systematically greater in specific areas, typically near major blood vessels. Significant effects of cardiac-related variability were found on average in 27.5 ± 8.0% of voxels. Strong influences were found along the vertebrobasilar arterial system near the medial areas of the brain, along the middle cerebral artery near the anterior temporal lobes and in the insula, and along the anterior cerebral artery in the anterior interhemispheric fissure in the medial frontal lobes. Significant effects were also observed in the sigmoid transverse and superior sagittal sinus regions. These results identify regions in which fMRI will have reduced sensitivity due to increased signal variation produced by cardiac pulsatility.

INTRODUCTION

Functional magnetic resonance imaging (fMRI) relies on the differential magnetic properties of oxygenated and deoxygenated hemoglobin to detect the localized decrease of deoxyhemoglobin that accompanies the increase in tissue metabolism occurring during neuronal activity (Thulborn *et al.*, 1982; Kwong *et al.*, 1992; Ogawa *et al.*, 1992). Because the signal change due to cortical function is slight, typically ranging from 1 to 2%, extraneous signal variance unrelated to experimental manipulations can make it difficult to detect neural activity and is thus of primary importance to experiments conducted with fMRI.

Most fMRI studies rely on the assumption that the brain is a static physical system which undergoes no structural changes during the course of the experiment. However, evidence from previous studies on brain physiology during the cardiac cycle have suggested that this is not the case. Because of the finite cranial volume, the influx of pumped blood results in a dynamic interaction between the competing space requirements of the blood volume, cerebrospinal fluid (CSF) pools, and brain tissue. During the systolic phase of the cardiac cycle, the sudden pressure increase within the cerebral vasculature causes an intracranial pressure wave that moves along the cerebral arterial tree in a fraction of a second (Feinberg *et al.*, 1987; Greitz *et al.*, 1992; Greitz, 1993). As a result, the arteries expand, first in the frontal lobe and subsequently in the more posterior parts of the brain, to make room in the cranial cavity for the influx of new blood. Some studies have noted blood volume changes at the capillary level, with expansion of the precapillaries and compression of the venous capillaries during systole (Greitz, 1993). The force exerted on the parenchyma from the expanding vasculature leads to inward expansion of the brain during systole and forces CSF down through the foramen magnum (Feinberg, 1992; Greitz, 1993; Greitz *et al.*, 1997). There is also uniform bulk motion of the large brain regions during systole which during diastole slowly return to their initial shape and configuration (Poncelet *et al.*, 1992). Studies examining this motion have reported that the central structures such as the diencephalon and brain stem move in the caudal direction while the peripheral regions such as the major cerebral lobes and posterior cerebellar hemisphere move in the cephalic direction (Enzmann *et al.*, 1992).

These physical changes can have important implications for cognitive experiments done with fMRI. Bulk brain motion or changes in blood volume at the capillary level could cause widespread global fluctuations of measured signal intensity with the cardiac cycle. Large-vessel pulsatility may affect the measured signal intensity in the areas adjacent to the vessels, both by causing

1053-8119/99 $30.00

tissue movement and by producing an influx of unsaturated blood into the slice of interest. These causes of increased signal variation can reduce the ability to detect hemodynamic changes related to neural activity using fMRI. A number of correction schemes have been suggested, involving retrospective gating or selective band frequency filtering (Hu *et al.*, 1995; Biswal *et al.*, 1996). However, most cognitive fMRI studies do not utilize a method of cardiac-related noise reduction, in part because of the lack of information on the regional significance and magnitude of cardiac-related signal variance in the brain.

Our goal was to locate the areas which showed significant contributions of cardiac-related activity, determine the percentage signal change during the cardiac cycle, and assess the implication on the detection of cognitive activity in these regions. Because typical whole-brain acquisition rates are much lower than the heart rate, aliasing makes direct observation of cardiac-induced signal changes difficult. In order to overcome this problem we used an adaptation of a previously described retrospective gating method (Hu *et al.*, 1995). By recording physiological data and whole-brain imaging data simultaneously and sorting the images according to the phase of the cardiac cycle at the time of acquisition we were able to estimate the signal change induced by the cardiac cycle throughout the brain.

The results are highly consistent across subjects and suggest that reduced sensitivity due to cardiac-induced noise in the blood oxygen level-dependent (BOLD) signal is systematically greater in specific areas, typically near major blood vessels and CSF pools. This signal change can be several times greater than that produced in response to typical cognitive paradigms. This source of error variance decreases the ability to detect BOLD signal changes due to neural activation in these regions.

MATERIALS AND METHODS

Subjects

Six healthy right-handed volunteers (two females, four males, age range 22–40 years) participated in this study. All were free of neurological or psychiatric illness. All subjects gave written informed consent.

Data Acquisition

Imaging was done on a 1.5-T MRI scanner (GE Signa, Milwaukee, WI) with a standard head coil. Gradient echoplanar scanning was used to produce 20–24 contiguous axial slices, scanned in an interleaved order, covering the entire cerebral cortex and the superior portion of the cerebellum (slice thickness 5.0 mm, repetition time (TR) = 3000 ms, echo time (TE) = 40 ms, flip angle 90°, field of view 24 cm, matrix 64 × 64, 96 repetitions per time series). For each subject, four series of whole-brain images were obtained while subjects were at rest. The cardiac cycle was monitored using a fiber optic photo pulse sensor (GE Signa) placed on the right index finger to measure the blood oxygenation level. The time at which 50% of the average peak blood oxygenation level amplitude was reached was used as an index of the onset of each cardiac cycle. A computer interfaced to the scanner recorded both the cardiac cycle and the slice acquisition times.

For all studies, high-resolution fast spoiled gradient recalled echo structural images were acquired at the same locations as the echoplanar images to provide detailed anatomic information (slice thickness 5.0 mm, TR = 14.1 ms, TE = 5.4 ms, flip angle 20°, matrix 256 × 256). For four of the subjects high-resolution 2D time-of-flight magnetic resonance angiography images were also acquired to provide information on cerebral vascular anatomy (slice thickness 2.5 mm, TR = 40 ms, TE = 4.1 ms, flip angle 60°, matrix 256 × 256).

Data Analysis

Between-scan movement was corrected with Automatic Image Registration (AIR) software which used an iterative method that minimized the ratio of voxel intensities between different time points (Woods *et al.*, 1992). Images were spatially smoothed in-plane with a Gaussian filter (FWHMx = 1.4 voxels (5.25 mm), FWHMy = 1.4 voxels). Statistical analyses were restricted to brain voxels with adequate signal intensity by selecting voxels with an average intensity of at least 10% of the maximum value across voxels.

Because the image acquisition rate (0.33 Hz) is much lower than the heart rate (1 Hz), aliasing makes it difficult to determine the cardiac-induced signal changes. These changes were analyzed by retrospectively sorting the images according to the phase of the cardiac cycle at their acquisition time. This allowed for the estimation of the signal intensity changes for each voxel during the cardiac cycle. This type of gating strategy, briefly described below, has been used successfully in cardiac imaging, in CSF flow velocity imaging, and more recently in a K-space physiological artifact correction method for fMRI (Lenz *et al.*, 1989; Bohning *et al.*, 1990; Nitz *et al.*, 1992; Hu *et al.*, 1995).

First, the relative phase of the cardiac cycle at the acquisition time of each slice is determined using the formula

$$\theta = \frac{T_s - T_a}{T_b - T_a},$$

where T_s represents the time of slice acquisition, T_a represents the onset time of the heartbeat just prior to the slice acquisition, and T_b represents the onset time

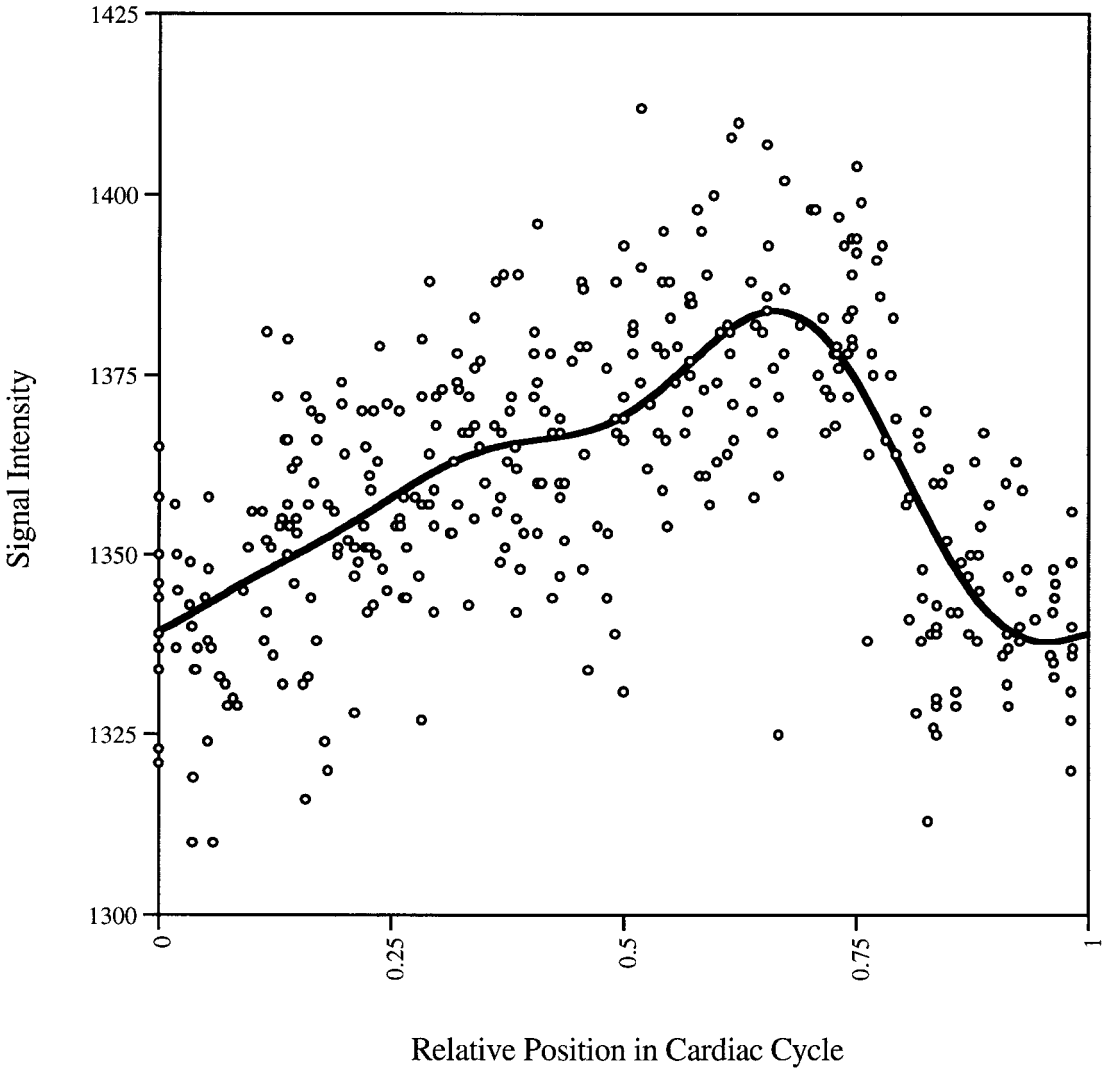

FIG. 1. Graph of the estimated signal change over the cardiac cycle for a voxel found in the area of the insula. There was considerable variation in the shape of these graphs for different voxels. Four series of 96 time points were pooled. The line represents the fit to the seven-term Fourier series. Its maximum and minimum values were used to calculate percentage signal change.

of the heartbeat just after the time of slice acquisition. Since different time points for any given slice location are acquired at different phases of the cardiac cycle, by pooling the data from all four series of scans, multiple observations of the signal intensity of each voxel over the entire cardiac cycle were obtained. To get an estimate of the shape of this cycle-induced change, the data for each voxel are fit to the seven-term Fourier series (Fig. 1),

$$f(\theta) = a_0 + \sum_{n=1}^{3} (a_n \cos(n\theta) + b_n \sin(n\theta)).$$

This gating strategy assumes that although the time interval between consecutive heartbeats may vary during the course of the experiment, each heart cycle follows the same general pattern, which is expanded or

TABLE 1

Distribution of Cardiac-Induced Variability

% Change	% of voxels	% Variance reduced
0.1–1.0	11.09 ± 4.10	10.51 ± 0.30
1.0–2.0	6.75 ± 1.69	19.87 ± 1.60
2.0–3.0	3.03 ± 0.77	24.85 ± 2.49
3.0–4.0	1.79 ± 0.53	26.10 ± 3.72
4.0–5.0	1.11 ± 0.33	28.03 ± 3.49
5.0–6.0	0.74 ± 0.16	29.93 ± 2.83
6.0–7.0	0.52 ± 0.07	32.29 ± 4.41
7.0–8.0	0.39 ± 0.09	32.78 ± 4.71
8.0+	2.12 ± 0.43	44.50 ± 5.76

Note. The proportion of voxels showing varying levels of percentage signal change induced by the cardiac cycle. For the voxels within each level, the proportion of signal variance attributable to the cardiac cycle and removed is also shown. The values shown are averaged over the six subjects studied.

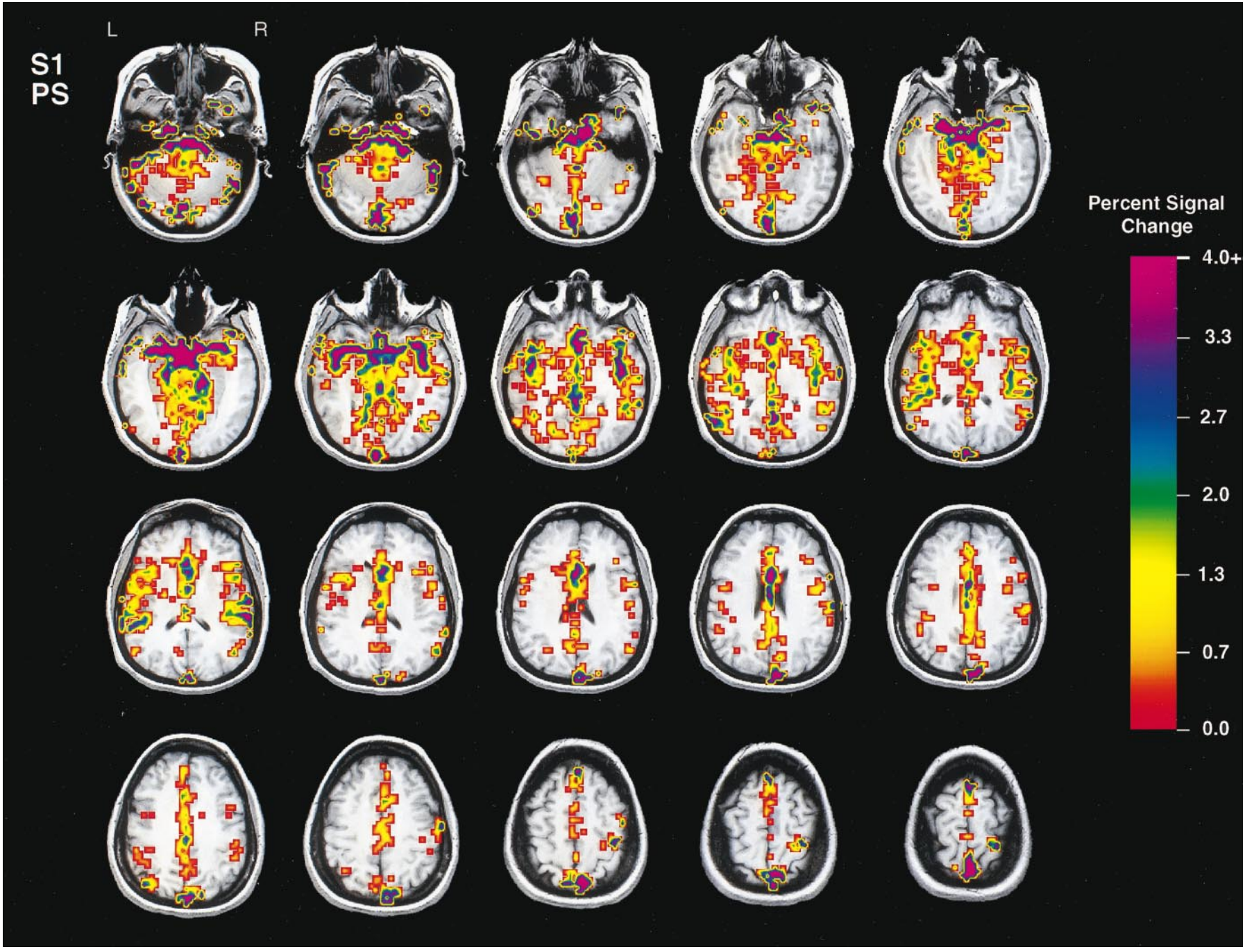
L
R
S1
PS
Percent Signal
Change
4.0+
3.3
2.7
2.0
1.3
0.7
0.0

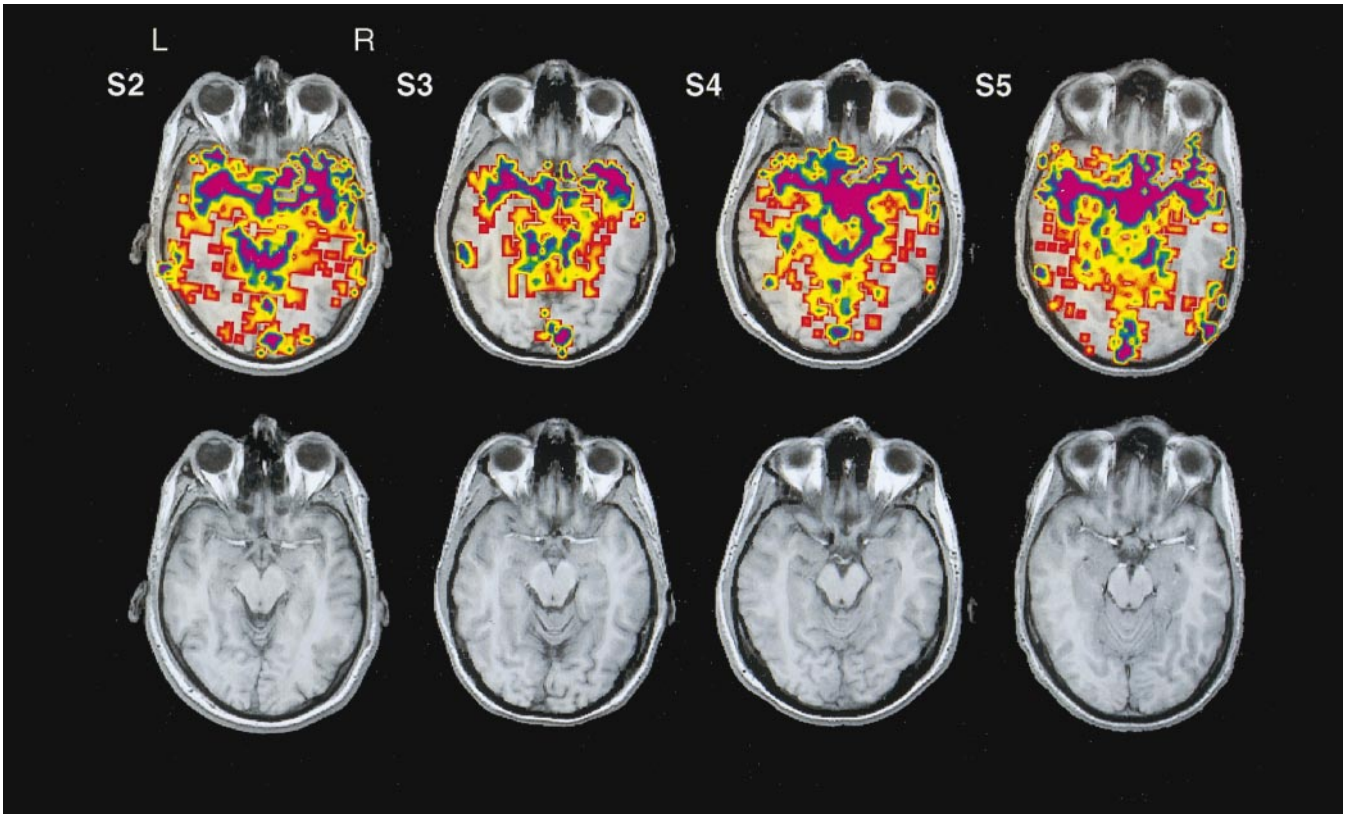

FIG. 3. Selected slices from four subjects showing a high degree of correspondence in the areas affected by cardiac activity across subjects. Pixels shown in color indicate regions demonstrating significant cardiac-related signal changes. Overlaid pixel colors have been scaled to reflect percentage signal change according to the color table shown in Fig. 2. The second row shows the same anatomical images shown above without the overlaid colors.

contracted in proportion to the interbeat time interval. Thus, the signal intensity changes for any voxel are directly related to the phase of the cardiac cycle. Also, because the systolic pulse does not necessarily reach the index finger and the brain simultaneously, the boundary points of the estimated cyclic signal changes are somewhat arbitrary. Differences in these times could cause the estimated cycle to be shifted.

When the four series of scans for each subject were combined, ANCOVA was used to factor out series variance caused by run-to-run shifts in signal mean intensity. The Durbin–Watson test for autocorrelation was performed on voxels showing a high degree of cardiac-related variability in order to confirm that the residuals of the fitted model were effectively independent (Bowerman *et al.*, 1990). Whole-brain statistical maps were then generated using an F test at each voxel to test the significance of the null hypothesis that signal change was uncorrelated with cardiac phase. These F values were in turn converted to Z scores. Regions of interest were located by identifying clusters of contiguous voxels which all exceeded a statistical threshold ($Z > 3.09$) and then calculating the probability for each cluster that a volume of that spatial extent could occur anywhere in the imaged brain volume by chance ($P < 0.001$) (Friston *et al.*, 1994). For the voxels that were contained within significant clusters, the percentage signal change over one cardiac cycle was computed using the fitted curves. This was defined as the percentage difference between the maximum and the minimum values of the fitted Fourier function for each voxel.

For the subjects for whom magnetic resonance angiography was acquired, the locations of the significant clusters were compared to that of the cerebral vasculature.

RESULTS

The average resting heart rate was 60 ± 5 beats/min and the within-subject interbeat time interval had an

FIG. 2. The full volume of a typical subject showing a topographical display of the percentage signal change during the cardiac cycle. Pixels shown in color indicate regions demonstrating significant cardiac-related signal changes. Overlaid pixel colors have been scaled to reflect percentage signal change according to the color table shown.

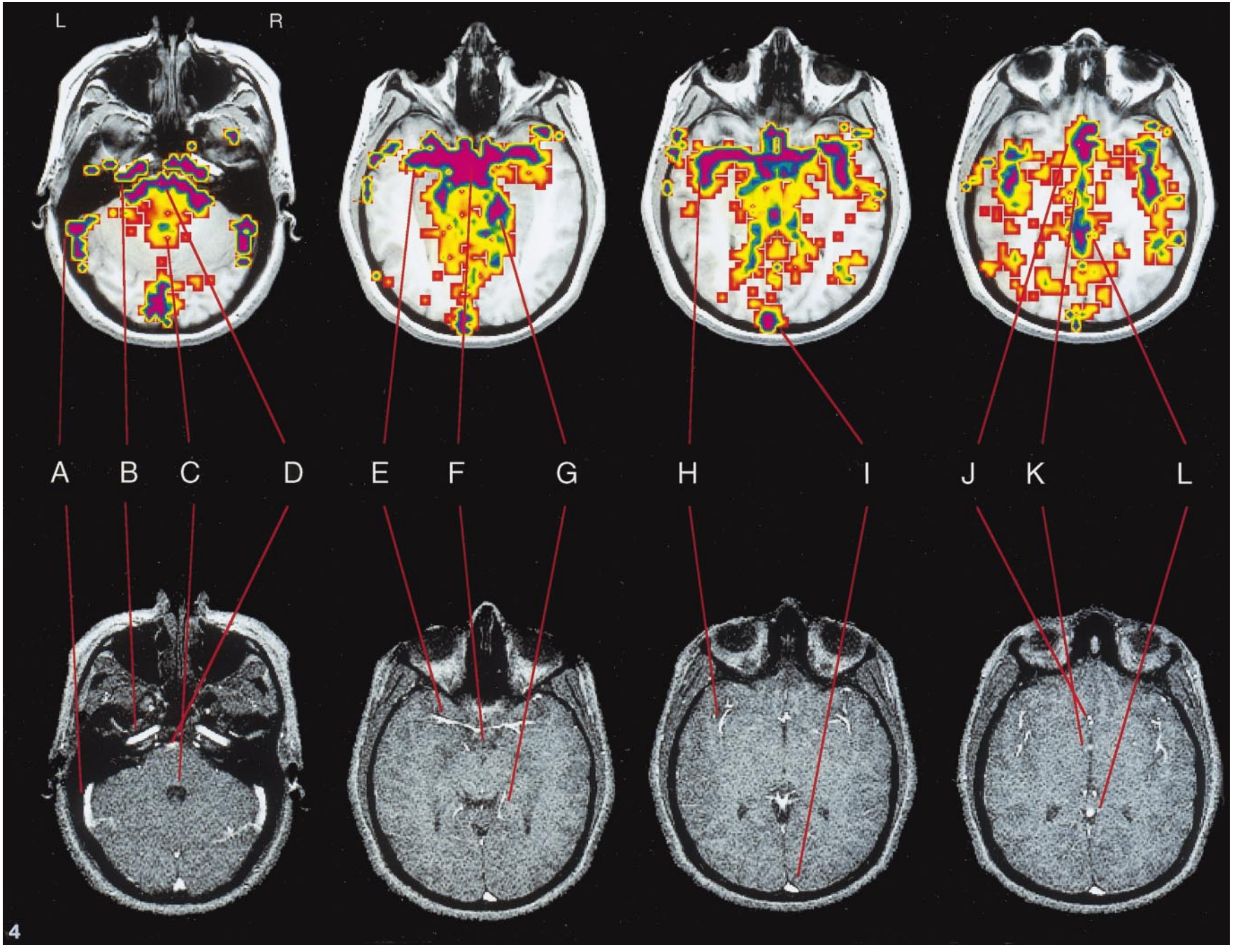
L
R
A
B
C
D
E
F
G
H
I
J
K
L
4

average standard deviation of approximately 6%. Significant cardiac-related signal changes were observed in 27.5 ± 8.0% of voxels across all subjects. Table 1 shows the distribution of significant signal changes observed and the proportion of signal variance that could be attributed to the cardiac cycle. All subjects showed areas of high cardiac-induced signal change that were localized to the regions proximal to the major blood vessels and their main branches. Figure 2 shows the full volume of a representative subject with voxels demonstrating significant cardiac-related signal changes shown in color. The color indicates the estimated percentage signal change induced by the cardiac cycle. Figure 3 shows percentage signal change maps for selected slices of subjects 2 through 5 to illustrate the high degree of correspondence between the areas showing significant change in different subjects.

Figure 4 shows a comparison of selected slices from subject 1 with the cerebral vasculature as determined by magnetic resonance angiography. In the vertebrobasilar circulation, strong influences were found proximal to the basilar artery (D) in the medial areas of the brain stem and proximal to the posterior cerebral branches (G) along the parahippocampal gyrus. In the internal carotid system strong influences were found bilaterally along the main trunk of the middle cerebral artery (H) with signal change noted in the superior temporal gyrus and insula. Strong influences were also observed within the interhemispheric fissure along the pathway of the anterior cerebral artery (J) and its pericallosal and callosomarginal branches producing signal change in the medial areas of the rectus, subcallosal, and cingulate gyri.

Although most regions of strong cardiac-correlated signal change were near the major arterial vessels, cardiac-induced variability was also noted in tissue along the superior sagittal sinus (I); in the medial areas of the lingual gyrus, cingulum, and precuneus; and in tissue along the sigmoid transverse sinus on the outer border of the cerebellar cortex. Small effects were also observed near CSF pools such as the third and fourth ventricles.

DISCUSSION

In this paper we have presented a topographical analysis of the effects of cardiac activity on fMRI. The results indicate that heartbeat introduces substantial regionally specific signal variance that is highly consistent across subjects in both location and magnitude. The areas exhibiting cardiac-related signal changes are generally proximal to the major arterial and venous structures and make up approximately one-quarter of the cerebral volume. Because these signal changes can be equal to or greater than those produced by cortical activity, the ability to detect signal changes due to neural activation would be decreased in these specific regions.

Several other studies have also noted the influence of cardiac activity on fMRI signal (Weisskoff *et al.*, 1993; Hu *et al.*, 1995; Biswal *et al.*, 1996; Jezzard *et al.*, 1996). Jezzard *et al.* (1996) performed a power spectrum analysis on the time series of selected voxels taken from an EPI data set (1.5 T, TR = 200 ms, TE = 40 ms) and observed peaks at the cardiac frequency and its harmonics. Similar results were observed by Biswal *et al.* (1996) using a gradient-echo EPI sequence (1.5 T, TE = 40 ms, TR = 1000 ms). Weisskoff *et al.* (1993), using a single-shot EPI sequence (1.5 T, TE = 50 ms, TR = 133 ms) to view a slice oblique along the calcarine fissure, found moderate cardiac influences in V1 cortical areas and stronger ones in the sagittal sinus and ventricles. More recently, Hu *et al.* (1995), performing a retrospective analysis on EPI K-space data (4.0 T, TR = 300 ms, TE = 30 ms), noted significant cardiac-correlated fluctuations in both the phase and the magnitude of the raw MR data.

This signal variation can have several effects. Large areas of signal change such as within the insula can effectively hide or mask the changes due to neural activity which are typically on the order of 1 to 2%. For example, variance due to the cardiac cycle would reduce a t test comparing activated and baseline conditions by approximately 15% when that cardiac-related variance accounts for 25 to 30% of the total signal variance. (For a simple experiment comparing two conditions, the reduction of the t test statistic is inversely proportional to the square root of $1 - p$ where p is the fraction of the variance arising from cardiac noise). The hippocampus, an area which has proven difficult to study with fMRI, shows clear influences from cardiac activity due to its proximity to the posterior cerebral artery. Small areas of high signal change, such as those found throughout the temporal lobe, could cause a continuous area of neural activity to appear as several distinct regions (Biswal *et al.*, 1996).

Because the areas showing high signal variation have a strong correspondence to the locations of the

FIG. 4. Comparison of selected functional slices (top slices) from one subject (S1) with the cerebral vasculature as examined by magnetic resonance angiography (bottom slices). The overlaid pixel colors on the functional slices have been scaled to reflect percentage signal change according to the color table shown in Fig. 2. There is a strong correspondence of tissue areas showing significant cardiac-related signal change to the locations of major blood vessels and CSF pools (A—transverse sinus, B—carotid artery, C—fourth ventricle, D—basilar artery, E—main trunk of middle cerebral artery (MCA), F—circle of Willis (entire region), G—posterior cerebral artery, H—branch of MCA, I—superior sagittal sinus, J—anterior cerebral artery, K—third ventricle, L—inferior sagittal sinus).

major blood vessels, the data suggest that cardiac-driven signal change is due mostly to vascular pulsations; possibly through in-flow enhancement caused by the introduction of unsaturated blood into the imaged slice, through flow dephasing between the excitation pulse and the readout, or through oblique flow displacement and misregistration artifact caused by the shifting locations of blood vessels, brain tissue, and CSF. In-flow enhancement and flow dephasing can produce, respectively, an increase and decrease in signal intensity concomitant with the cardiac pressure wave. Movement can produce signal fluctuations around vessels, by varying the partial volumes within voxels for different tissue types (gray and white matter, blood vessels, and CSF). Because the exact timing difference between the arrival of the pressure wave to the finger and to the cerebral tissue is not known, it is difficult to state with certainty if there is a predominant cause of variation. However, the fact that considerable variation was seen throughout the brain in both the direction and the course of voxel signal intensity changes during the cardiac cycle suggests that more than one factor plays a role.

Little induced variation is seen in tissue distant from major vessels, suggesting that cardiac-induced changes in blood oxygenation at the capillary level are not a significant cause of signal variance in fMRI. This also suggests that cardiac-related bulk brain tissue motion is not great enough to introduce significant signal variation as this would also be present in tissue distant from major vascular structures. This finding is not surprising as the maximum displacement of brain tissue during the cardiac cycle has been estimated to be about 0.04 mm in the parietal lobes and 0.09 mm in the frontal lobes (Enzmann *et al.*, 1992). It is surprising, however, that significant signal change was not observed at the brain periphery as movement of this magnitude can produce a 1 to 2% signal change at this border. A closer look at the data before statistical analysis revealed that cardiac-correlated signal change of approximately this magnitude seemed to be present in the peripheral parenchyma of most subjects. However, this change did not achieve significance, possibly because of the high signal noise typically found in the peripheral tissue arising from movement due to other causes. It is possible that cardiac-induced signal change is also present at other tissue borders but is of insignificant magnitude compared to variation produced by other sources of motion.

As one moves to more superior regions of the brain the effects of cardiac activity are not as strong. This is expected due to the smaller vessels present in these regions and the dampening that occurs along the cerebral circulatory system, reducing the periodic pressure and velocity fluctuations within the minor arterial branches. The notable variation in signal observed around the sinuses is not surprising due to the pulsatile blood flow that is unique to the cranial veins and occurs as the result of compression from the pulsating brain tissue (Greitz, 1993).

A fundamental assumption in this analysis is that the cardiac cycle follows the same inherent pattern regardless of the interbeat time interval. Although this assumption has been used in the past, it is only an approximation. In general, differences in the time interval between beats is associated more by time variation in the diastolic portion than in the systolic. For this reason a model which assumes equal contraction of all parts of the cycle is not completely accurate and can result in underestimated values of percentage signal change and significance.

Currently, there are several available options for reducing cardiac-related signal fluctuations at long TRs. Hu *et al.* (1995) used a retrospective gating procedure similar to that used in this study to remove phase and magnitude fluctuations in the K-space data. Biswal *et al.* (1996) approached this task by using band-reject digital filters at the cardiac frequency and its estimated aliased frequencies. Both of these methods resulted in significant decreases in signal variability. Alternatively, based on the results from this study, it seems feasible that a retrospective gating procedure can be applied directly to the reconstructed image-space data. By including the Fourier terms of the cardiac model within the general linear model typically used for time series analysis, cardiac-induced variability can be characterized simultaneously with data analysis. This may be preferable to removing physiological variation as a preprocessing step since it minimizes the misattribution of variance in cases in which the paradigm and the heartbeat are correlated.

CONCLUSIONS

These results suggest that reduced sensitivity due to cardiac-induced variation in the BOLD signal is greater in specific areas, typically near major blood vessels and CSF pools. This introduction of signal error variance is highly consistent across subjects in both location and magnitude and may impede the detection of cognitive activity in these regions. Of particular interest are the effects seen in the medial and anterior temporal lobes which have implications for studies of visual recognition, semantic knowledge, and episodic memory. Correction of this source of error variance will increase the ability to detect signal changes due to neural activation in these regions.

REFERENCES

Biswal, B., DeYoe, E. A., and Hyde, J. S. 1996. Reduction of physiological fluctuations in fMRI using digital filters. *Magn. Reson. Med.* **35:**107–113.

Bohning, D. E., Carter, B., and Liu, S. 1990. PC-based system for retrospective cardiac and respiratory gating of NMR data. *Magn. Reson. Med.* **16:**303–316.

Bowerman, B. L., and O'Connell, R. T. 1990. *Linear Statistical Models: An Applied Approach*, Vol. 2. PWS–Kent, Boston.

Enzmann, D. R., and Pelc, N. J. 1992. Brain motion: Measurement with phase-contrast MR imaging. *Radiology* **185:**653–660.

Feinberg, D. A. 1992. Modern concepts of brain motion and cerebrospinal fluid flow. *Radiology* **185:**630–632.

Feinberg, D. A., and Mark, A. S. 1987. Human brain motion and cerebrospinal fluid circulation demonstrated with MR velocity imaging. *Radiology* **163:**793–799.

Friston, K. J., Worsley, K. J., Frackowiak, R. S., Mazziotta, J. C., and Evans, A. C. 1994. Assessing the significance of focal activations using their spatial extent. *Hum. Brain Mapp.* **1:**210–220.

Greitz, D. 1993. Cerebrospinal fluid circulation and associated intracranial dynamics. A radiologic investigation using MR imaging and radionuclide cisternography. *Acta Radiol.* **34**(Suppl. 386):1.

Greitz, D., Greitz, T., and Hindmarsh, T. 1997. A new view on the CSF-circulation with the potential for pharmacological treatment of childhood hydrocephalus. *Acta Paediatr.* **86**(2):125–132.

Greitz, D., Wirestam, R., Franck, A., Nordell, B., Thomsen, C., and Stahlberg, F. 1992. Pulsatile brain movement and associated hydrodynamics studied by magnetic resonance phase imaging. *Neuroradiology* **34:**370–380.

Hu, X., Le, T., Parrish, T., and Erhard, P. 1995. Retrospective estimation and correction of physiological fluctuation in functional MRI. *Magn. Reson. Med.* **34:**202–212.

Jezzard, P., and Song, A. 1996. Technical foundations and pitfalls of clinical fMRI. *NeuroImage* **4:**S63–S75.

Kwong, K. K., Belliveau, J. W., Chesler, D. A., Goldberg, I. E., Weisskoff, R. M., Poncelet, B. P., Kennedy, D. N., Hoppel, B. E., Cohen, M. S., Turner, R., Cheng, H. M., Brady, T. J., and Rosen, B. R. 1992. Dynamic magnetic resonance imaging of human brain activity during primary sensory stimulation. *Proc. Natl. Acad. Sci. USA* **89:**5675–5679.

Lenz, G. W., Haack, E. M., and White, R. D. 1989. Retrospective cardiac gating: A review of technical aspects and future directions. *Magn. Reson. Med.* **7:**445–455.

Nitz, W. R., Bradley, W. G., Watanabe, A. S., Lee, R. R., Burgoyne, B., O'Sullivan, R. M., and Herbst, M. D. 1992. Flow dynamics of cerebrospinal fluid: Assessment with phase-contrast velocity MR imaging performed with retrospective cardiac gating. *Radiology* **183:**395–405.

Ogawa, S., Menon, R. S., Tank, D. W., Kim, S. G., Merkle, H., Ellerman, J. M., and Urgubil, K. 1992. Intrinsic signal changes accompanying sensory stimulation: Functional brain mapping with magnetic resonance imaging. *Proc. Natl. Acad. Sci. USA* **89:**5951–5955.

Poncelet, B. P., Wedeen, V. J., Weisskoff, R. M., and Cohen, M. S. 1992. Brain parenchyma motion: Measurement with cine echoplanar MR imaging. *Radiology* **185:**645–651.

Thulborn, K. R., Waterton, J. C., Matthews, P. M., and Radda, G. K. 1982. Oxygenation dependence of the transverse relaxation time of water protons in whole blood at high fields. *Biochem. Biophys. Acta* **714:**265–270.

Weisskoff, R. M., Baker, J., Belliveau, J., Davis, T. L., Kwong, K. K., Cohen, M. S., and Rosen, B. R. 1993. Power spectrum analysis of functionally-weighted MR data: What's in the noise? Proc. SMRM, 1st Annual Meeting, p. 1407.

Woods, R. P., Cherry, S. R., and Mazziotta, J. C. 1992. Rapid automated algorithm for aligning and reslicing PET images. *J. Comput. Assisted Tomogr.* **16**(4):620–633.